第 48 卷 第 9 期/2021 年 5 月/中国激光 研究论文

中国激光

高重复频率窄脉宽单频激光器

张雅楠[1,2]，孟俊清[1*]，王明建[1]，于真真[1]，陈卫标[1]

[1]中国科学院上海光学精密机械研究所空间激光传输与探测技术重点实验室，上海 201800；

[2]中国科学院大学，北京 100049

摘要 介绍了一种基于反射式体布拉格光栅(RBG)的高重复频率窄脉宽的固体单频激光器。该激光器采用激光二极管端面泵浦的方式，Nd∶YVO_4 晶体为增益介质，磷酸氧钛铷(RTP)晶体对为电光调 Q 开关，RBG 为输出镜，在光学腔长为 65.7 mm 的谐振腔内，锁定了波长 1064.355 nm 的单频激光输出，其在 10 kHz 的重复频率下，脉冲宽度为 1.3 ns、平均功率为 1.68 W、光束质量 $M_x^2=1.22$ 和 $M_y^2=1.18$，可应用于空间主动光电遥感技术中。

关键词 激光器；固体激光器；体布拉格光栅；高重复频率；窄脉宽；单频

中图分类号 TN248.1 **文献标志码** A **doi**：10.3788/CJL202148.0901005

1 引 言

激光雷达作为一种空间主动光电遥感技术，对高精度三维成像、高垂直分辨率对地探测以及高时空分辨率的深空探测具有非常重要的意义[1-4]。对于传统的星载和高空机载激光雷达，多采用低重复频率、高脉冲能量的激光信号和线性光电探测技术，但存在功耗高、体型大、距离分辨率低等问题[5]。单光子探测技术的发展简化了激光雷达系统，提高了探测灵敏度和探测效率，给激光雷达带来了飞跃的发展，但是也要求不同性能参数的激光信号：1)采用高重复频率的激光脉冲，通常为 kHz 量级以上，提高采样频率，更精确地描绘采样目标；2)具有更窄的脉冲宽度，减小探测误差，提高激光雷达的探测精度；3)具有更窄的激光线宽，配合相应的窄带滤光片，降低背景噪声对探测器的影响，提高探测系统灵敏度[6]。

2015 年，NASA 发射到国际空间站的云、气溶胶运输系统激光雷达，采用 CATS(Cloud-Aerosol Transport System)探测载荷，在工作一模式下可发射重复频率为 5 kHz 的 1064、532 nm 激光，线宽分别为 100 pm@1064 nm、45 pm@532 nm，脉冲宽度 <10 ns，单脉冲能量低至 2 mJ[7-8]；2018 年，NASA 发射的 Ice Sat-2 卫星，采用光子计数探测，搭载激光测高载荷 ATLAS(Advanced Topographic Laser Altimeter System)，可实现重复频率为 10 kHz、脉冲宽度为 1.5 ns、单脉冲能量为 0.2～1.2 mJ 可调的 532 nm 激光[9-11]。近年来我国也开展了关于空间单光子探测激光雷达的相关研究：2016 年中国科学院上海光学精密机械研究所设计了一种基于光子计数技术的远程测距激光雷达，激光器输出激光重复频率为 1 kHz，脉冲宽度 10 ns，单脉冲能量为 15 mJ[12]。2017 年，华东师范大学研制了 100 光束光子计数激光雷达，使用 532 nm 的激光器重复频率为 10 kHz，脉冲宽度为 600 ps，单脉冲能量为 0.3 μJ[13]。

在此基础上，为了实现更远距离的探测，提高激光雷达光源重复频率、脉冲能量，降低脉冲宽度、谱线宽度是目前的发展趋势。本文搭建了一种结构紧凑的高重复频率、高脉冲能量、窄脉宽输出的单频激光器，可应用在基于单光子探测技术的空间主动探测激光雷达方面。

2 实验装置及原理分析

2.1 窄脉冲理论分析

根据 Degnan 的调 Q 理论[14]，输出激光的半峰全宽(FWHM)为

收稿日期：2020-10-15；**修回日期**：2020-11-11；**录用日期**：2020-11-27

*E-mail：jqmeng@siom.ac.cn

$$t_p=\frac{t_r}{L}\left\{\left[\frac{\ln z}{z}\right]\left\{\frac{1}{1-\left[\frac{z-1}{z\ln z}\right]\left\{1+\ln\left[\frac{z\ln z}{z-1}\right]\right\}}\right\}\right\},\tag{1}$$

式中：$t_r=2l_r/c$ 为腔内的往返时间；l_r 为谐振腔腔长；c 为真空中的光速；L 为腔内往返损耗；无量纲参数 $z=2g_0l/L$，g_0 为增益介质的小信号增益系数，l 为增益介质的长度。

对于端面泵浦的激光系统而言，增益介质的小信号增益系数又可以表示为[15]

$$g_0=\eta_Q\eta_S\eta_B\sigma_{21}\tau P_P/h\nu_P\pi\omega_P^2 l,\tag{2}$$

式中：η_Q、η_S、η_B 分别为量子效率、斯托克斯因子、交叠效率；σ_{21}、τ 为增益介质的受激辐射截面、上能级寿命；P_P、ν_P、ω_P 分别为泵浦光的功率、频率、光斑半径。

综合上述可以看出，增益介质的 $\sigma_{21}\tau$、谐振腔腔长 l_r、泵浦光功率 P_P、腔内往返损耗 L 是影响脉冲宽度的因素。根据计算：在常用的红外晶体材料中，Nd∶YVO_4 晶体的 $\sigma_{21}\tau$ 相对较高，因此选用其作为激光增益介质对于实现窄脉冲输出有着明显的优势[16]；另外，腔长越短且泵浦功率越大，激光脉冲宽度越窄。根据实验条件，将表 1 相关实验参数值代入脉冲宽度表达式并画出示意图 1。可以看出，本次实验要产生脉冲宽度 1 ns 左右的激光脉冲，在保证谐振腔内光学元件互不干扰且安全工作的条件下，腔长需缩短至 3～5 cm，且泵浦功率需大于 9 W。

表 1　实验参数值

Table 1　Experimental parameter value

Parameter	Value	Parameter	Value
η_Q	0.90	h /(J·s)	6.63×10^{-34}
η_S	0.76	ν_P/ s^{-1}	3.7×10^{14}
η_B	0.8	ω_P/μm	200
σ_{21} /cm^2	15.6×10^{-19}	l /mm	10
τ /μs	100	L	0.34

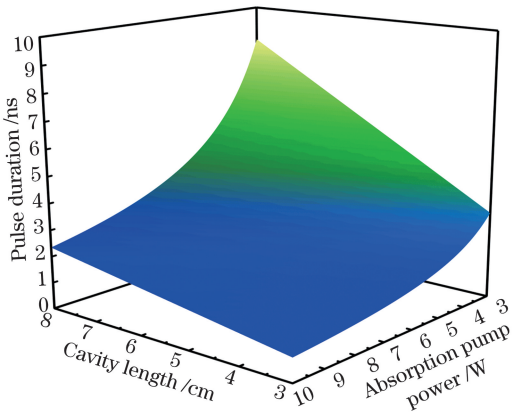

图 1　脉冲宽度与腔长、吸收泵浦功率的关系

Fig. 1　Relationship between pulse width and cavity length and absorbed pump power

2.2　实验装置

激光器实验装置如图 2 所示，采用带尾纤输出的中心波长为 808 nm 的半导体激光器，光纤的芯径、数值孔径分别为 200 μm、0.22，可实现功率 0～15 W 的可调连续输出。准直聚焦系统为两个焦距分别为 15 mm、23 mm 的平凸镜组合，将 808 nm 泵浦光聚焦耦合到增益晶体中，其焦点处实际光斑半径为 300 μm。镀 808 nm 高透膜和 1064 nm 高反膜的 0°平面全反镜 M1，与耦合输出元件反射式体布拉格光栅(RBG)形成平平腔结构，谐振腔物理腔长为 48 mm。其中 RBG 尺寸为 5 mm×5 mm×12.5 mm，图 3 是归一化透过率对与波长的关系示意图，在中心波长 1064.36 nm 处的透过率为 34%，FWHM 为 0.04 nm，在谐振腔中同时起到锁定波长的作用。增益介质 Nd∶YVO_4 晶体尺寸为 3 mm×3 mm×10 mm，沿 a 轴切割，掺杂原子数分数为 0.25%，前后表面都镀有 808 nm 和 1064 nm 增透膜。采用水冷方式散热，将用铟箔包裹的 Nd∶YVO_4 晶体放置在通水热沉中，与底板相连并利用水箱进行温度控制，温度固定为 20 ℃。实验中采用加压式调 Q 方式，高频高压电光驱动信号的上升沿为 1 ns，重复频率为 10 kHz，电压幅值为

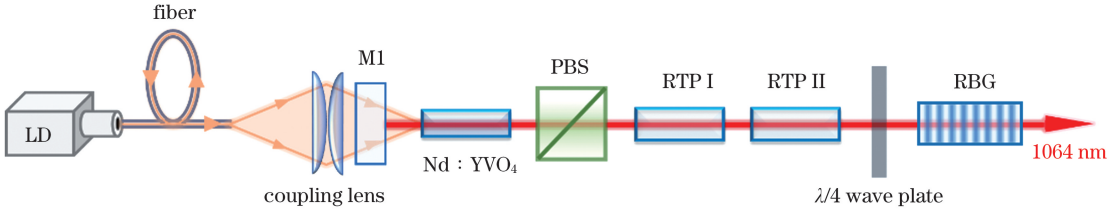

图 2　激光器结构图

Fig. 2　Experimental setup of laser

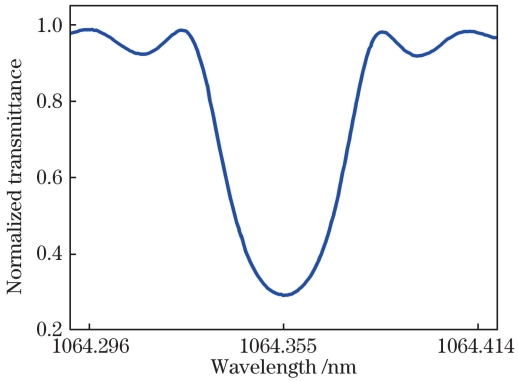

图 3 反射式体布拉格光栅的衍射效率曲线图

Fig. 3 Spectral profile of a collimated beam diffracted by RBG

2.3 kV；6 mm×6 mm×6 mm 的偏振分光棱镜 PBS 为起偏器，4 mm×4 mm×14 mm 的磷酸氧钛铷(RTP)晶体对为电光调 Q 元件，与 1/4 波片三者共同构成激光器的 Q 开关：旋转调节 1/4 波片，在 RTP 晶体未加电压时，经过起偏器 PBS 的线偏振光，在谐振腔内往返经过 RTP 晶体、1/4 波片后，返回到 PBS 的激光的偏振方向与初始线偏光方向垂直，无法通过 PBS 形成激光振荡，即谐振腔处于关门状态；当对 RTP 晶体加 1/4 波电压时，RTP 作用相当于 1/4 波片，经过 PBS 的偏振光两次经过 RTP 晶体、1/4 波片，再次返回 PBS 时，不改变偏振光的状态，谐振腔开门，实现调 Q 脉冲的振荡输出。

3 分析与讨论

按照上述装置搭建激光器系统光路，LD 泵浦模块为连续光输出。使用 Coherent Power Max PM10 30 W 功率计测试得到 1064 nm 激光的输出平均功率随 LD 泵浦功率变化的曲线如图 4 所示，

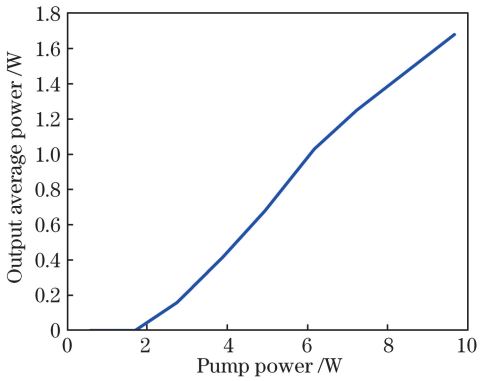

图 4 激光器输出平均功率与 LD 泵浦功率的关系

Fig. 4 Relationship between laser output average power and pump power

在温度为 20 ℃，LD 工作电流为 6.2 A(泵浦光功率为 9.67 W)时，得到平均功率为 1.68 W 的激光输出，光-光转换效率为 17.4%；并记录了在 3 h 内的输出功率变化情况，如图 5 所示，平均输出功率为 1.689 W，功率抖动的标准差为 5.422 mW，功率不稳定性为 0.32%。

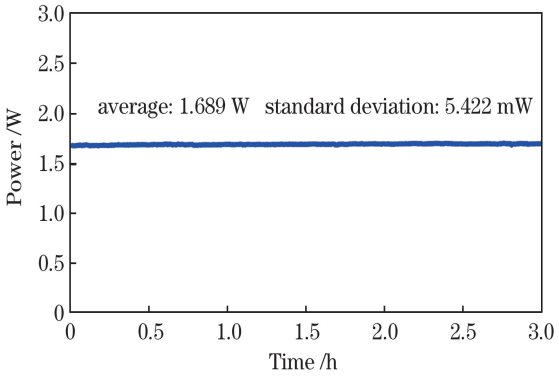

图 5 激光器输出光功率稳定性测量

Fig. 5 Stability measurement of laser output power

采用上升沿响应速率为 60 ps 的 PIN 光电管对脉冲进行采集，Teledyne LeCroy 公司型号为 MSO 104MXs-B 的示波器(带宽为 1 GHz，采样率为 20 GS/s)进行显示，获得的脉冲波形如图 6 所示，可以看到脉冲波形光滑，脉冲宽度约为 1.3 ns。使用 YOKOGAWA 公司的光谱仪对输出激光波长波形进行测量，得到如图 7 所示的中心波长为 1064.355 nm 的激光输出，锁定波长与 RBG 中心波长一致，谱线宽度测试达到光谱仪的分辨率极限，即光谱线宽小于 0.05 nm。使用 High Finesse WS7 波长计对输出波长及线宽进行测量，如图 8 所示，输出光线宽为 1.0 pm。根据纵模间隔公式 $\Delta\lambda=\lambda_0^2/(2l')$[17]，在本次实验中光学谐振腔腔长 l' 为 65.7 mm 的条件下的纵模间隔为 8.6 pm，比输出

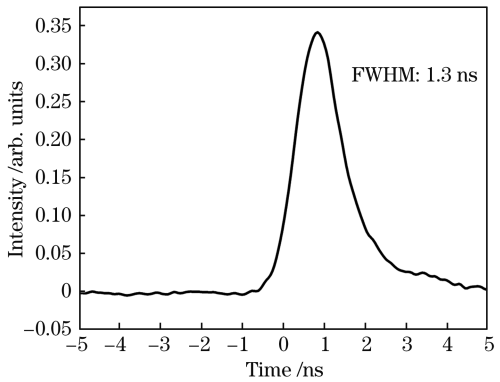

图 6 激光器脉冲波形图

Fig. 6 Pulse profile of laser

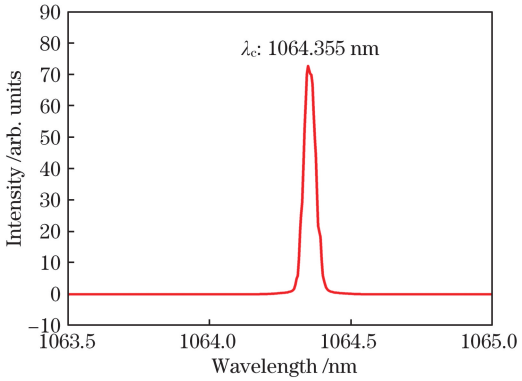

图 7　激光输出光谱图

Fig. 7　Laser output spectrum

激光线宽大，所以输出光脉冲为单纵模。这是由于 RBG 在 0.04 nm 的线宽范围内仅能容纳 4～5 个纵模，且不同纵模的选择透过率不同，在谐振腔中相互竞争，其中衍射效率最高的 1064.355 nm 附近的纵模，在激光腔内往返振荡的过程中得到放大并输出。采用 CCD 和德国 CINOGY TECHNOLOGIES 激光光束分析仪对输出光斑及光束质量进行测量，如图 9 所示，两个方向的光束质量因子分别为 $M_x^2=1.22$、$M_y^2=1.18$。

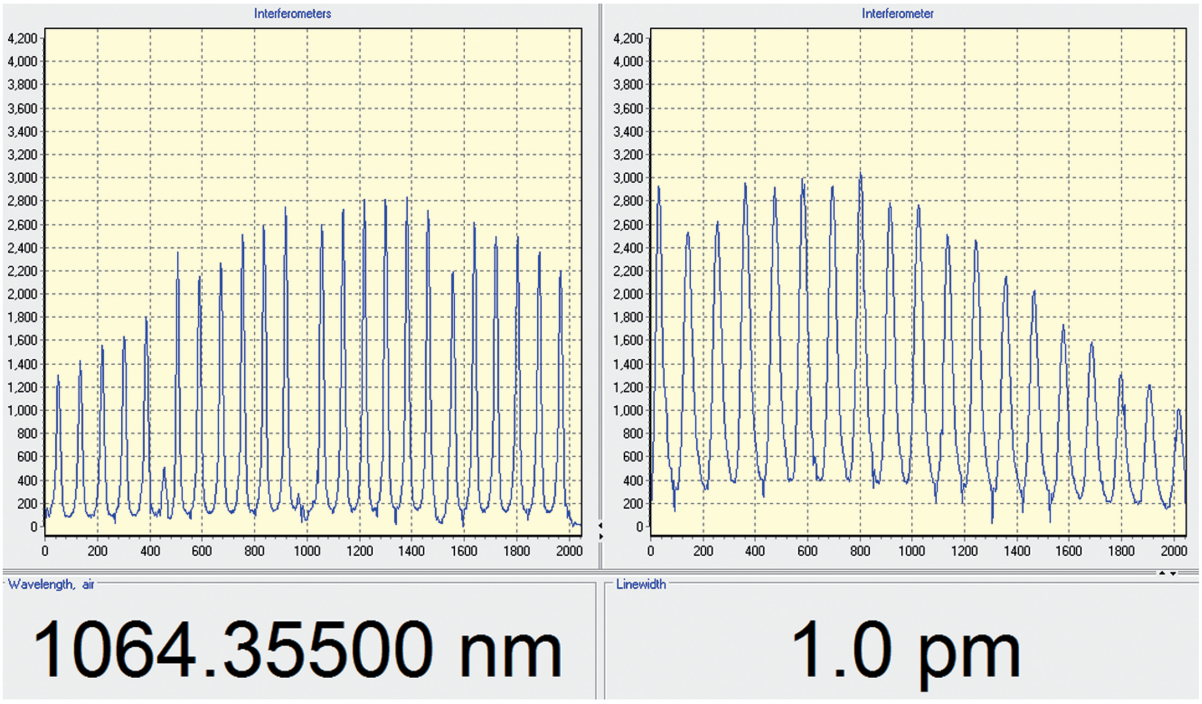

图 8　输出激光波长与线宽图

Fig. 8　Wavelength and line width of output laser

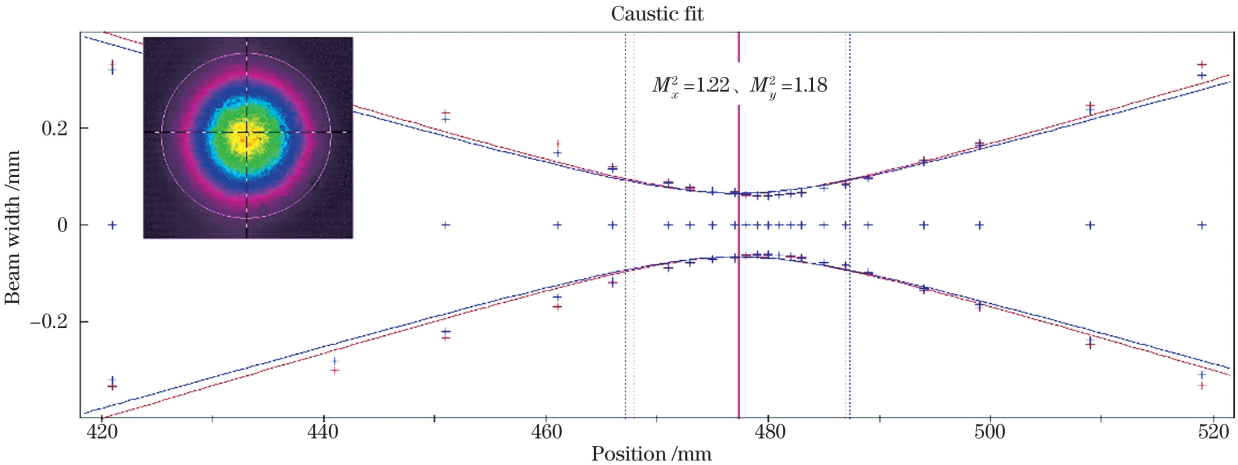

图 9　输出激光光斑和光束质量

Fig. 9　Beam profile and beam quality of output laser

4 结 论

介绍了一种高重复频率窄脉宽的单频固体激光器。采用 RTP 电光调 Q 方式，在 LD 端面泵浦下，RBG 锁定了波长为 1064.355 nm 的单频激光输出，在工作频率为 10 kHz 时，其脉冲宽度为 1.3 ns，单脉冲能量为 168 μJ，光束质量因子 $M_x^2=1.22$、$M_y^2=1.18$。该激光器结构紧凑，实现了高重复频率下的窄脉宽、窄线宽、大能量激光输出，可以作为空间探测的激光雷达发射光源使用，也可以作为主振荡功率放大(MOPA)系统的种子源进行放大，以实现更远距离的探测。

参 考 文 献

[1] Liu B, Yu Y, Jiang S. Review of advances in LiDAR detection and 3D imaging [J]. Opto-Electronic Engineering, 2019, 46(7): 190167.
刘博, 于洋, 姜朔. 激光雷达探测及三维成像研究进展[J]. 光电工程, 2019, 46(7): 190167.

[2] Shu R, Kong W. Current status and development of space-based active opto-electronics remote sensing technology[J]. Aerospace Shanghai, 2019, 36(3): 1-14.
舒嵘, 孔伟. 空间主动光电遥感现状及发展[J]. 上海航天, 2019, 36(3): 1-14.

[3] Yu Z Z, Hou X, Zhou C Y. Progress and current state of space-borne laser altimetry [J]. Laser & Optoelectronics Progress, 2013, 50(2): 020006.
于真真, 侯霞, 周翠芸. 星载激光测高技术发展现状[J]. 激光与光电子学进展, 2013, 50(2): 020006.

[4] Zhang J, Zhang D, Liu H W, et al. Actively Q-switched fiber laser with narrow linewidth, narrow pulse width, and high repetition rate [J]. Chinese Journal of Lasers, 2020, 47(1): 0101002.
张骥, 张东, 刘昊炜, 等. 一种窄线宽的高重复频率窄脉宽主动调 Q 光纤激光器[J]. 中国激光, 2020, 47(1): 0101002.

[5] Wang A Y, Tao Y L, Li X, et al. Design and test of high repetition frequency photon counting lidar prototype[J]. Laser & Infrared, 2017, 47(7): 803-807.
王遨游, 陶宇亮, 李旭, 等. 高重频光子计数激光雷达样机设计及测距试验[J]. 激光与红外, 2017, 47(7): 803-807.

[6] Liu Q, Meng J Q, Zu J F, et al. High repetition frequency narrow pulse electro-optically Q-switched laser for space applications [J]. Chinese Journal of Lasers, 2017, 44(6): 0601005.
刘琪, 孟俊清, 祖继锋, 等. 适于空间应用的高重复频率窄脉冲电光调 Q 激光器[J]. 中国激光, 2017, 44(6): 0601005.

[7] Chuang T, Burns P, Brooke Walters E, et al. Space-based, multi-wavelength solid-state lasers for NASA's cloud aerosol transport system for international space station (CATS-ISS) [J]. Proceedings of SPIE, 2013, 8599: 85990N.

[8] McGill M J, Yorks J E, Stanley Scott V, et al. The cloud-aerosol transport system (CATS): a technology demonstration on the international space station [J]. Proceedings of SPIE, 2015, 9612: 96120A.

[9] Neumann T A, Martino A J, Markus T, et al. The Ice, Cloud, and Land Elevation Satellite-2 mission: a global geolocated photon product derived from the Advanced Topographic Laser Altimeter System [J]. Remote Sensing of Environment, 2019, 233: 111325.

[10] Burns P M, Sawruk N W, VanTuijl A, et al. Design validation for ICESat2 space-based laser transmitter [J]. Proceedings of SPIE, 2014, 9218: 92181G.

[11] Yao J Q, Tang X M, Li G Y, et al. Cloud detection of laser altimetry satellite ICESat-2 and the related algorithm [J]. Laser & Optoelectronics Progress, 2020, 57(13): 131408.
么嘉棋, 唐新明, 李国元, 等. 激光测高卫星 ICESat-2 云检测及其相关算法[J]. 激光与光电子学进展, 2020, 57(13): 131408.

[12] Luo Y, He Y, Geng L M, et al. Long-distance laser ranging lidar based on photon counting technology [J]. Chinese Journal of Lasers, 2016, 43(5): 0514001.
罗远, 贺岩, 耿立明, 等. 基于光子计数技术的远程测距激光雷达[J]. 中国激光, 2016, 43(5): 0514001.

[13] Li Z, Wu E, Pang C, et al. Multi-beam single-photon-counting three-dimensional imaging lidar[J]. Optics Express, 2017, 25(9): 10189-10195.

[14] Degnan J J. Theory of the optimally coupled Q-switched laser [J]. IEEE Journal of Quantum Electronics, 1989, 25(2): 214-220.

[15] Koechner W. Solid-state laser engineering [M]. Beijing: Science Press, 2002.
克希耐尔. 固体激光工程[M]. 北京: 科学出版社, 2002.

[16] Lu J, Ding J Y, He Y, et al. High repetition rate sub-nanosecond dual-wavelength solid-state laser for airborne lidar[J]. Laser & Optoelectronics Progress, 2018, 55(8): 082804.
陆俊, 丁建永, 贺岩, 等. 机载激光雷达用高重复频率亚纳秒双波长全固态激光器[J]. 激光与光电子学

进展, 2018, 55(8): 082804.

[17] Hu X, Cheng D J, Wang S B, et al. Single-frequency Nd∶YVO$_4$ laser based on reflective Bragg grating combined with Fabry-Perot etalon[J]. Acta Optica Sinica, 2019, 39(5): 0514002.
胡星, 程德江, 王思博, 等. 基于反射式布拉格光栅和 Fabry-Perot 标准具组合的 Nd∶YVO$_4$ 单频激光器[J]. 光学学报, 2019, 39(5): 0514002.

High Repetition Frequency Narrow Pulse Width Single Frequency Laser

Zhang Yanan[1,2], Meng Junqing[1*], Wang Mingjian[1], Yu Zhenzhen[1], Chen Weibiao[1]

[1] *Key Laboratory of Space Laser Communication and Detection Technology, Shanghai Institute of Optics and Fine Mechanics, Chinese Academy of Sciences, Shanghai* 201800, *China*;

[2] *University of Chinese Academy of Science, Beijing* 100049, *China*

Abstract

Objective As a space active photoelectric remote sensing technology, lidar is of great significance to high-precision three-dimensional imaging, ground detection with high vertical resolution, and deep space exploration with high spatio-temporal resolution. For traditional spaceborne and high-altitude airborne lidars, laser signals with low repetition rate and high pulse energy and linear photoelectric detection technology were mostly used, which had problems such as high power consumption, large size, and low surface resolution. The development of single-photon detection technology can simplify the lidar system, and improve the detection sensitivity and detection efficiency. However, it also requires laser signals with different performance parameters. Laser with high repetition rates can increase the sampling frequency and describe the sampling target more accurately. And the laser signal with a narrower pulse width can reduce the detection error and improve the detection accuracy of the lidar. And the narrower linewidth laser, combined with the corresponding narrowband filter, can reduce the influence of background noise on the detector and improve the sensitivity of the detection system. In this paper, we report a compact single-frequency laser with high repetition rate, high pulse energy, and narrow pulse width output. We hope that our laser will be helpful to space active detection lidar based on single-photon detection technology.

Methods In order to achieve narrow pulse laser output, electro-optic Q-switch is selected to obtain narrow pulses under 10 ns and generate high peak power laser. According to the theory of electro-optic Q-switched laser, the factors affecting the pulse width are analyzed: Nd∶YVO$_4$ crystal with higher $\sigma_{21}\tau$ value is selected to obtain a higher small signal gain; the cavity length is shortened and the pump power is increased to obtain a narrower laser pulse. In order to achieve a narrow linewidth laser output, a volume Bragg grating mode selection method is used to build a solid single-frequency laser. The laser is end-pumped by a continuous-wave laser diode. The semiconductor laser with a pigtail output has a center wavelength of 808 nm, which can realize an adjustable continuous output with a power of 0–15 W. The core diameter and numerical aperture of the fiber are 200 μm and 0.22. The collimating and focusing system is a combination of two plano-convex lenses with focal lengths of 15 mm and 23 mm, respectively. The 808 nm pump light is focused on the gain crystal. The actual spot radius of the focal point is about 300 μm. The 0° total reflection plane mirror M1 coated with 808 nm high-transmittance film and 1064 nm high-reflection film forms a flat cavity structure with the coupling output element reflective volume Bragg grating (RBG), and the physical cavity length is 48 mm. The polarization beam splitting is used as a polarizing element. The rubidium titanyl phosphate (RTP) crystal pair is used as an electro-optic Q-switch. PBS, RTP and the 1/4 wave plate together constitute the Q-switch of the laser. It adopts a voltage-increased electro-optic Q-switched method, and is driven by a high-frequency and high-voltage signal to realize the on and off switch of the optical circuit, forming a Q-switched giant pulse output.

Results and Discussions At a repetition frequency of 10 kHz, when the pump power is 9.67 W, a laser output with an average power of 1.68 W is obtained (Fig. 4). The power instability within 3 h is 0.32% (Fig. 5). The output laser pulse width is 1.3 ns, and the pulse waveform is smooth (Fig. 6). The output wavelength is 1064.355 nm, and the line width is 1.0 pm (Fig. 8). According to the longitudinal mode interval formula $\Delta\lambda = \lambda_0^2/(2l')$, the longitudinal mode interval is 8.6 pm in the condition of 65.7 mm optical cavity length in this experiment, which is larger than line width of the output laser. So the laser realizes single longitudinal mode output.

The beam quality factor of two directions is $M_x^2 = 1.22$ and $M_y^2 = 1.18$ (Fig. 9).

Conclusions A single-frequency solid-state laser with high repetition rate and narrow pulse width is introduced in this paper. The laser is end-pumped by a continuous-wave laser diode, Nd∶YVO_4 crystal as gain medium, the RTP crystal pair as the electro-optic Q-switch, and RBG as output mirror. In a resonant cavity with an optical cavity length of 65.7 mm, the single-frequency laser output with a wavelength of 1064.355 nm is locked. And at a repetition frequency of 10 kHz, the laser has a pulse width of 1.3 ns, an average power of 1.68 W, and the beam quality of $M_x^2 = 1.22$ and $M_y^2 = 1.18$. The laser has a compact structure and achieves a narrow pulse width, a narrow line width, and a large energy laser output at a high repetition rate. It can be used as a laser radar emission source for single-photon detection, and can also be used as a seed source of the main oscillation power amplification system for amplification to achieve more long-distance detection.

Key words lasers; solid-state laser; volume Bragg grating; high repetition frequency; narrow pulse width; single frequency

OCIS codes 140.3460; 140.3480; 140.3540; 140.3580